

Variability in equatorial Pacific sea surface topography during the verification phase of the TOPEX/POSEIDON mission

Antonio J. Busalacchi

Laboratory for Hydrospheric Processes, NASA Goddard Space Flight Center, Greenbelt, Maryland

Michael J. McPhaden

Pacific Marine Environmental Laboratory, NOAA, Seattle, Washington

Joel Picaut

Groupe Surveillance Trans-Océanique du Pacifique, ORSTOM, Noumea, New Caledonia

O.R.S.T.O.M. Fonds Documentaire
N° 42 803
Cote B Ex 1

M

P20

Abstract. As part of the verification phase of the TOPEX/POSEIDON mission, 10-day gridded fields of altimeter data derived from TOPEX geophysical data records are compared with 10-day gridded fields of dynamic height derived from more than 60 moorings of the Tropical Ocean and Global Atmosphere-Tropical Atmosphere Ocean (TOGA-TAO) array in the equatorial Pacific Ocean. Access to TAO data in real time permits the first 500 days of the TOPEX/POSEIDON mission to be placed in the context of complementary, in situ measurements of surface winds, sea surface temperatures, and upper ocean thermal structure, as well as the time history of these variables prior to launch. Analysis of the space-time structure in the TOPEX and TAO surface topography data indicates sea level variability primarily due to equatorial Kelvin wave activity generated by intense wind bursts west of the date line in association with the 1991-1993 El Niño. Cross correlations between the two data sets are generally >0.7, with RMS differences <4 cm. However, for reasons not fully understood, correlations drop to <0.5 in certain regions off the equator in the eastern Pacific, and RMS differences can be >5 cm north of the equator in the central and eastern Pacific.

1. Introduction

During the 5-year Geosat altimeter mission the largest year to year changes in sea level, on basin to global scales, were the order 15- to 20-cm sea level fluctuations in the tropical Pacific Ocean associated with the 1986-1987 El Niño event [Koblinsky, 1993]. The Geosat mission, originally intended for geodetic and mesoscale oceanographic applications, proved surprisingly successful at monitoring the El Niño-related equatorial wave propagation and the changes in equatorial zonal current across the entire low-latitude Pacific basin [Miller *et al.*, 1988; Picaut *et al.*, 1990; Delcroix *et al.*, 1991]. TOPEX/POSEIDON, with an improved RMS error budget of 9 cm for individual altimeter retrievals [Fu and Christensen, 1993], was designed for the expressed purpose of studying the large-scale ocean circulation. In view of the increased accuracy relative to Geosat and a mission design life of 5 years, a cautious optimism and anticipation existed prior to launch that the TOPEX/POSEIDON mission would also be able to monitor the evolution of a complete El Niño cycle.

The timing of the launch of TOPEX/POSEIDON in August 1992 was somewhat fortuitous since it occurred in the middle of the extended 1991-1992-1993 El Niño [Kousky, 1993; McPhaden, 1993]. Although this meant that the entire development (i.e., initiation, mature phase, and decay) of

this particular El Niño episode would not be captured, it did mean that significant sea level variability should be present across the entire equatorial Pacific basin during the initial verification phase of the mission. This variability was observed from in situ measurements provided by the Tropical Ocean and Global Atmosphere (TOGA)-Tropical Atmosphere Ocean (TAO) observing system. TOGA-TAO was designed to provide continuous, high-quality measurements in the equatorial Pacific waveguide for improved description, understanding, and prediction of short-term climate variability. In contrast to 1986-1987, when satellite altimeter measurements were compared with tide gauge observations from ~30 islands of the TOGA sea level network (mostly situated in the western tropical Pacific) and/or several TAO moorings [e.g., Cheney *et al.*, 1989; Wyrki and Mitchum, 1990; Koblinsky *et al.*, 1992; Delcroix *et al.*, 1994], the subsequent deployment of ~60 TAO surface moorings in the equatorial Pacific now permits monitoring dynamic height variability, among other quantities, on a real-time basis across the full width of the equatorial Pacific basin. Together with the TOGA expendable bathythermograph network and the TOGA surface velocity drifter network, no other portion of the world ocean is as densely instrumented and routinely monitored as the equatorial Pacific Ocean.

Thus the purpose of this paper is to examine the sea level variability described by TOPEX/POSEIDON measurements for the equatorial Pacific Ocean during the first 17 months of the mission. Our focus for comparison will be the dynamic topography computed from TOGA-TAO observations.

Copyright 1994 by the American Geophysical Union.

Paper number 94JC01638.
0148-0227/94/94JC-01638\$05.00



TAO Array

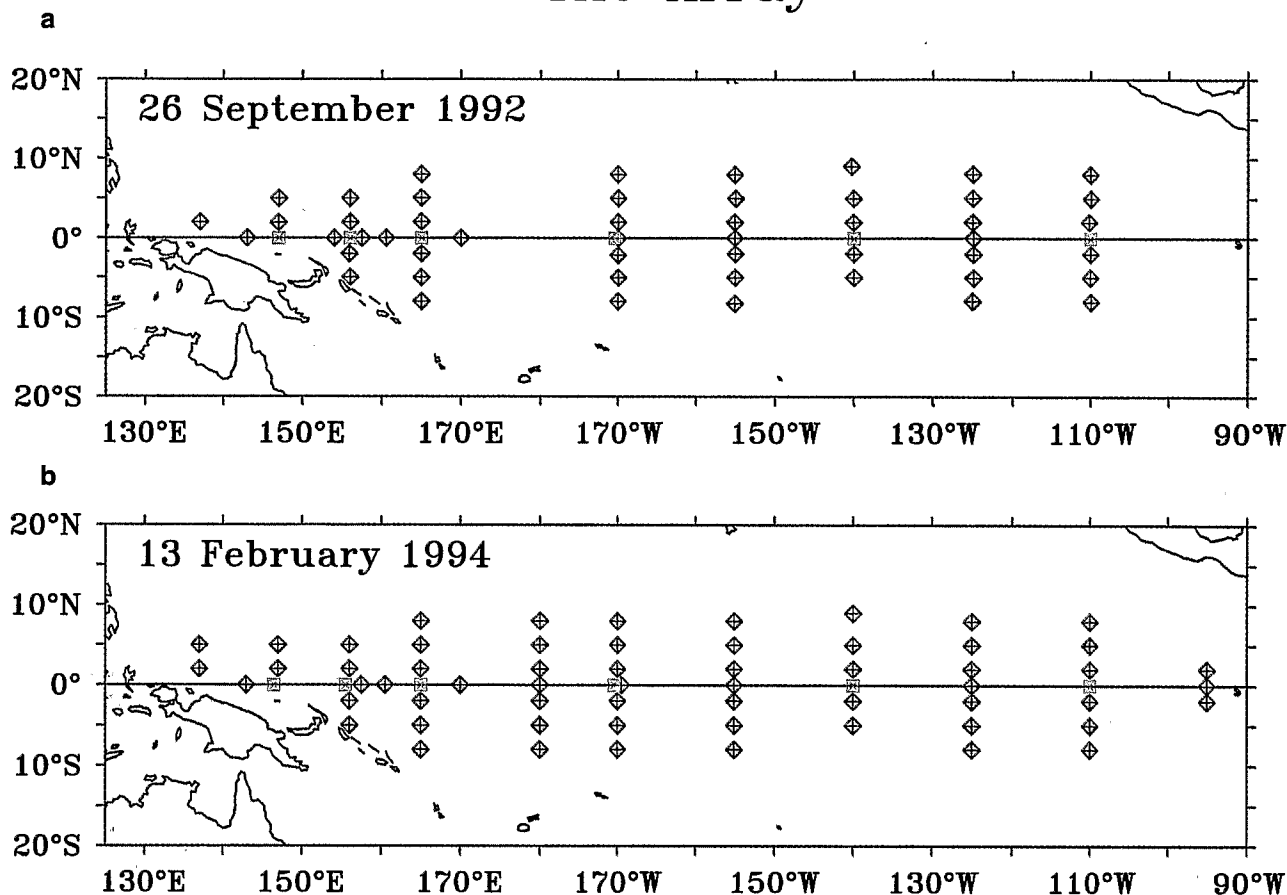


Plate 1. The Tropical Ocean and Global Atmosphere–Tropical Atmosphere Ocean (TOGA-TAO) array on (a) September 26, 1992 and (b) February 13, 1994. Autonomous Temperature Live Acquisition System (ATLAS) moorings (diamonds) and current meter (squares) moorings are indicated.

Other papers in this issue [e.g., Mitchum, this issue] will deal with intercomparisons of TOPEX/POSEIDON and tide gauge observations. The existence of the TOGA-TAO array will also allow us to interpret the initial TOPEX/POSEIDON measurements within the context of the 1991–1993 El Niño which occurred prior to, during, and after the verification phase. We will conclude with a discussion of the relative merits of these two measurement technologies in the post-TOGA era.

2. Data and Method of Analysis

2.1. TOPEX Altimeter

The TOPEX altimeter data to be used here are an enhanced geophysical data record (GDR) produced by the NASA Goddard Space Flight Center ocean altimetry group (courtesy of C. Koblynsky). In this data set the GDRs from the TOPEX project have been interpolated every 6 km to fixed points along track and referenced to the locations of the cycle 17 ground tracks. The tidal corrections applied are that of Ray *et al.* [1994]. The first 51 10-day cycles are considered here (September 26, 1992 to February 13, 1994). Ten-day fields of sea level anomalies relative to the mean over the first 506 days have been created by optimally interpolating the collinear data onto a $1^\circ \times 1^\circ$ grid using decorrelation scales of 15° zonally and 3° meridionally.

2.2. TOGA-TAO

The in situ data used in this study are from the multinational supported TOGA TAO array of Autonomous Temperature Line Acquisition System (ATLAS) and Profile Telemetry of Upper Ocean Currents (PROTEUS) moorings [McPhaden, 1993]. ATLAS is a taut-line surface mooring which measures winds, air temperature, relative humidity, sea surface temperature (SST), and subsurface temperature. Daily averages and occasional spot hourly data are telemetered to shore in real time via Service Argos [Hayes *et al.*, 1991]. Complete hourly time series of SST and meteorological data are internally recorded. PROTEUS moorings are of similar design to ATLAS moorings, except that daily averaged current profiles in the upper 250 m are telemetered to shore in real time from an acoustic Doppler current profiler mounted in the surface toroid [McPhaden *et al.*, 1991]. By the start of the first cycle of TOPEX/POSEIDON altimeter data (September 26, 1992) the TOGA-TAO array consisted of 56 moorings spanning approximately 8°N – 8°S , 110°W – 137°E ; by the end of cycle 51 (February 13, 1994), TAO consisted of 65 moorings between 95°W and 137°E (Plate 1 and Figure 1).

Daily averaged sea surface temperature and subsurface temperature from the TAO array are used to compute dynamic height of the sea surface relative to 500 dbar. (In the

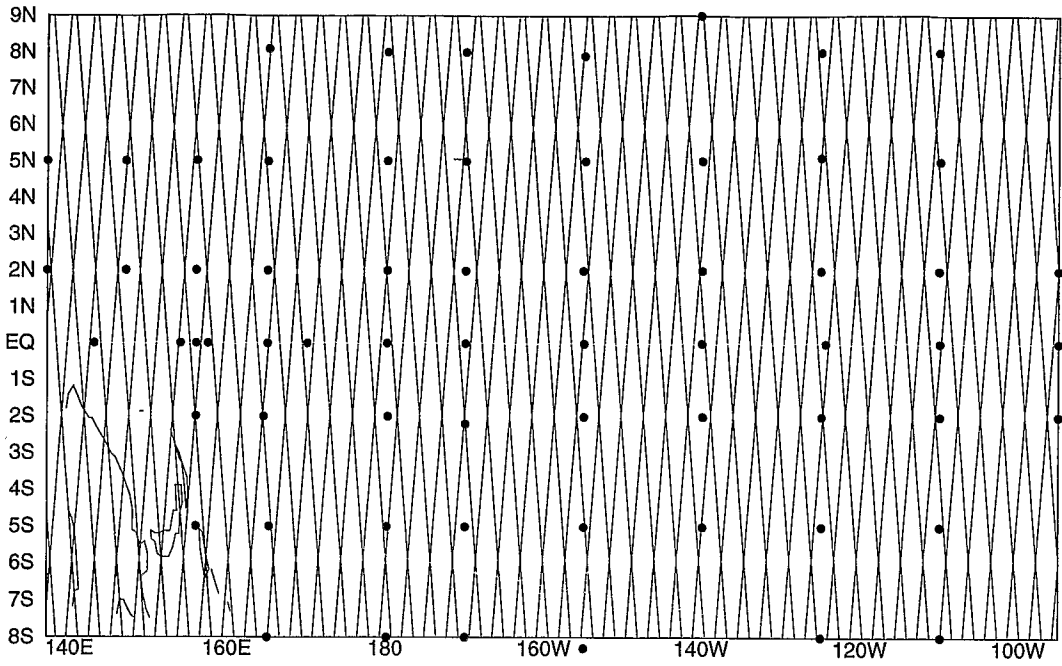


Figure 1. Location of the TOPEX/POSEIDON “ground” tracks relative to the mooring locations.

a Zonal Wind Anomalies ($m s^{-1}$)

b SST Anomalies ($^{\circ}C$)

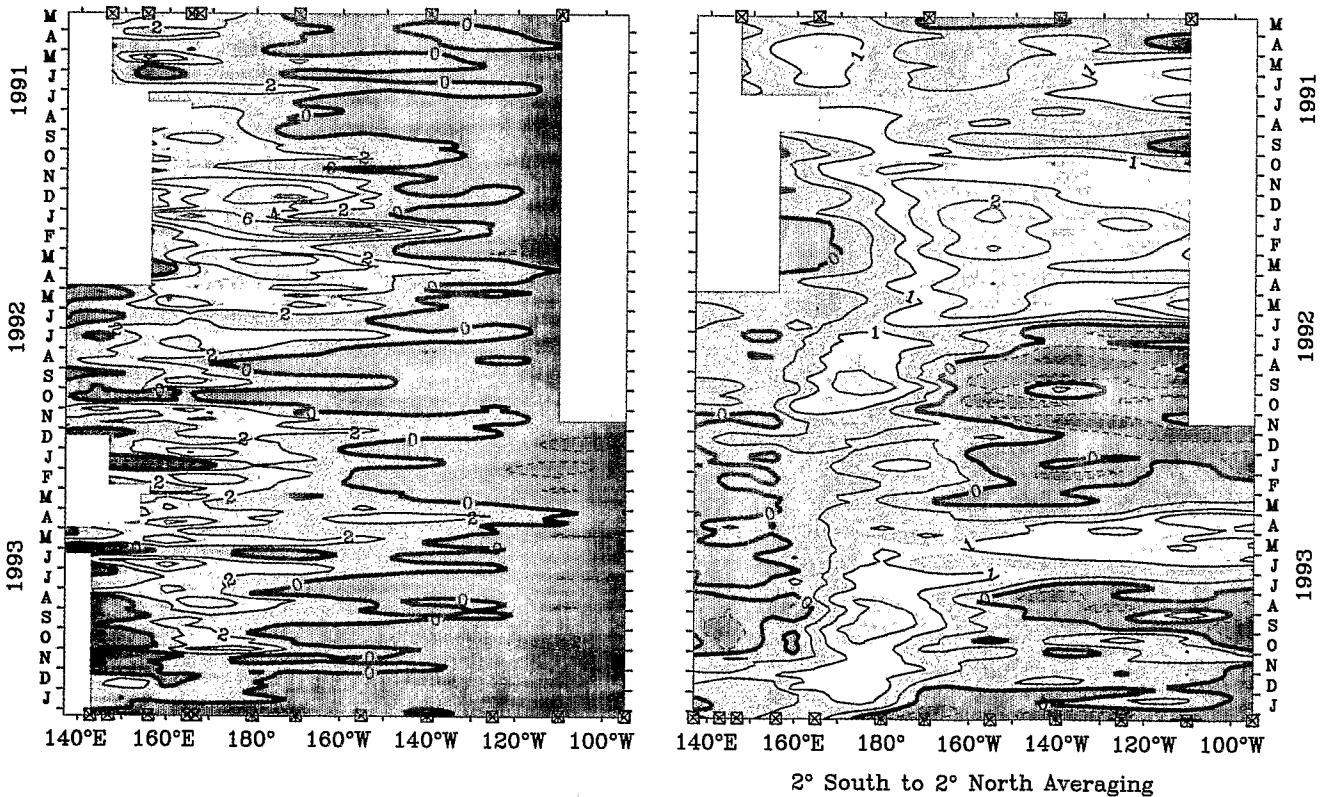


Plate 2. Time-longitude plots of (a) zonal wind anomalies and (b) sea surface temperature (SST) anomalies. Wind anomalies are relative to the Comprehensive Ocean-Atmosphere Data Set climatology [Woodruff *et al.*, 1987], and SST anomalies are relative to the Reynolds' [1988] climatology. Mooring data have been averaged latitudinally between 2°N and 2°S and processed to 5-day averages. The climatologies were interpolated to 5-day values using cubic splines. Symbols along the top abscissa indicate longitudes with data at the start of the period; symbols along the bottom abscissa indicate longitudes with data at the end of the period.

comparisons with the TOPEX altimeter data that follow the TAO dynamic height variability will be discussed in the context of dynamic height anomalies about the mean dynamic height for the study period.) Salinity information required for this calculation is derived from a mean temperature–salinity relationship based on the *Levitus* [1982] climatology. Use of the mean temperature–salinity relationship introduces an error of ~ 3 dynamic centimeters (dyn. cm) in the western Pacific and ~ 2 dyn. cm in the eastern Pacific based on sensitivity tests using 126 conductivity–temperature–depth (CTD) casts between 1°N – 1°S , 165°E (February 1986 to October 1992) and 80 CTD casts near 0° , 110°W (February 1979 to October 1991).

The choice of a 500-dbar reference level results in a loss of ~ 5 – 15% of the signal amplitude in the equatorial Pacific based on sensitivity tests using full water column CTD data. Losses at the higher end of this range (15%) characterize the western Pacific, where the thermocline is deep, while losses at the lower end (5%) characterize the eastern Pacific, where the thermocline is shallow. For root-mean-square (RMS) signal amplitudes of 5–6 dyn. cm these losses imply < 1 dyn. cm bias in the TAO-derived dynamic heights due to the choice of reference level. In addition, the relatively coarse vertical resolution of the TAO subsurface temperature data (e.g., 10 levels in the upper 500 m for ATLAS moorings) introduces about a 0.5-dyn. cm error in dynamic heights relative to more finely resolved CTD measurements. Temperature sensor instrumental errors on ATLAS and PROTEUS moorings are typically $< 0.1^{\circ}\text{C}$ [e.g., *McCarty and McPhaden*, 1993; *Freitag et al.*, 1994]. Assuming these errors are uncorrelated for different sensors at different levels, the expected error in 0/500 dbar dynamic height due to instrumental noise would be typically ~ 0.3 dyn. cm.

Taking all the above errors into account results in an expected error of ~ 3 – 4 dyn. cm in the western Pacific and ~ 2 – 3 dyn. cm in the eastern Pacific.

3. Climatic Context

The period encompassed by this study (September 1992 to February 1994) was characterized by large-scale climate anomalies associated with the 1991–1993 El Niño event (Plates 2 and 3) (see also *McPhaden* [1993] and *Kessler et al.* [1994]). Weak El Niño conditions began to develop in early 1991, but it was not until boreal fall of 1991 that persistent, basin-scale, warm SST anomalies $> 1^{\circ}\text{C}$ developed in the equatorial Pacific (Plate 2b). These warm anomalies amplified in association with a weakening of the trade winds over 50° – 60° of longitude in late 1991 to early 1992 (Plate 2a). This weakening was not monotonic but was punctuated by several westerly wind anomalies that extended progressively farther into the central and eastern Pacific. The response to these westerly wind events was a series of baroclinic equatorial Kelvin waves which propagated eastward at ~ 2.5 m s^{-1} [*Kessler et al.*, 1994] and lead to 10–15 dyn. cm oscillations in dynamic height in the central and eastern Pacific (Plate 3). By February to March 1992, dynamic heights were lower than normal by 20 dyn. cm in the western Pacific and higher than normal by ~ 20 dyn. cm in the eastern Pacific (Plate 3b). Thus dynamic height along the equator, which is typically ~ 50 dyn. cm higher in the west than in the east, was almost flat west of 140°W at this time (Plate 3a).

Dynamic height dropped sharply in the eastern Pacific

during boreal spring 1992, SST returned to normal in the cold tongue by June 1992, and by August 1992 the trade winds returned to normal strength in the central Pacific. These developments suggested that the El Niño might be coming to an end. However, intraseasonal westerly wind anomalies of a few meters per second continued to be prevalent west of the date line in late 1992 and early 1993, and these oscillations continued to excite eastward propagating Kelvin waves. In particular, westerly wind events during November 1992 to January 1993, which occurred during the TOGA–Coupled Ocean Atmosphere Response Experiment (COARE) intensive observing period [*Webster and Lukas*, 1992], lead to excitation of Kelvin waves which elevated dynamic heights by ~ 5 – 10 dyn. cm as they propagated along the equator to the eastern Pacific (e.g., Plate 3). These Kelvin waves, though smaller in amplitude than those observed in late 1991 and early 1992, were followed by a flare up of El Niño conditions in early 1993 (Plate 2b). The reemergence of large-scale warm SST anomalies the year following a major El Niño has no analog in the past 40 years for which reliable records exist to draw meaningful comparisons. However, this warming in the eastern Pacific cold tongue began to abate such that by July 1993, near-normal zonal winds, SSTs, and dynamic heights were observed along the equator in the eastern Pacific. On the other hand, near to and west of the date line, dynamic heights remained 5–20 dyn. cm lower than normal, westerly wind anomalies of a few meters per second persisted, and warm SST anomalies intensified to $> 1.5^{\circ}\text{C}$.

Monthly mean maps of dynamic height in the equatorial Pacific determined from TAO data allow for a detailed examination of spatial patterns of variability. The January 1993 map, for example (Plate 4), shows the mean equatorial ridge–trough structure in the meridional direction, with an equatorial trough centered near the equator, an equatorial ridge at $\sim 5^{\circ}\text{N}$, and a south equatorial ridge between 5° and 8°S west of 140°W [cf. *Wyrki and Kilonsky*, 1984]. This particular map also shows a reversal of the zonal dynamic height slope along the equator between 170° and 180°W in association with westerly wind anomalies of a few meters per second west of the date line. However, winds along the equator in the western Pacific were weak easterlies in an absolute sense, suggesting that the dynamic height reversal observed during this month is not in equilibrium with the local wind forcing. This disequilibrium is to be expected, given the degree to which dynamic height variability is affected by wave transients.

4. Intercomparison

In this section the space–time structure of the surface topography will be examined for both the TOPEX and TOGA–TAO data sets within $\sim 8^{\circ}$ of the equator. We wish to determine if the large-scale signals depicted by TOPEX during the first 506 days of the mission are consistent with those observed by the in situ TOGA–TAO network. Since the TAO array was designed, in part, to observe the excitation and propagation of equatorial wave activity in the tropical Pacific Ocean, particular attention will be given to the description of wave variability in the TOPEX data.

Anomalies in this section will be defined relative to the mean over 506 days encompassing cycles 1–51 of the TOPEX/POSEIDON mission (September 26, 1993 to Febru-

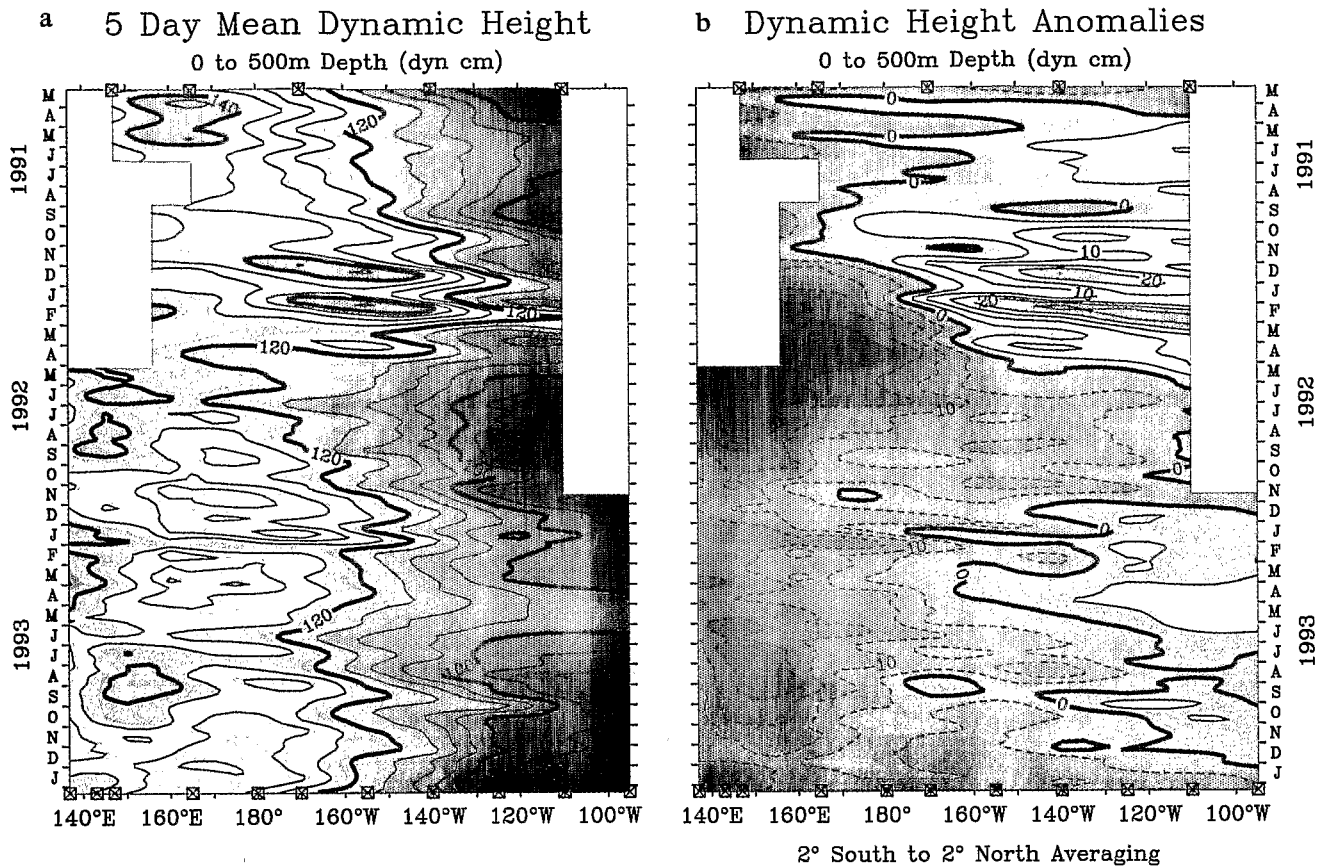


Plate 3. Time-longitude plots of (a) dynamic height and (b) dynamic height anomalies relative to 500 dbar. Anomalies are relative to a climatology derived from expendable bathythermograph data [Kessler, 1990] and Levitus [1982] mean temperature-salinity profiles. Mooring data have been averaged latitudinally between 2°N and 2°S and processed to 5-day averages. The climatologies were interpolated to 5-day values using cubic splines. Symbols along the top abscissa indicate longitudes with data at the start of the period; symbols along the bottom abscissa indicate longitudes with data at the end of the period.

TAO Monthly Mean Dynamic Height (0/500m,dyn-cm) and Winds ($m s^{-1}$)

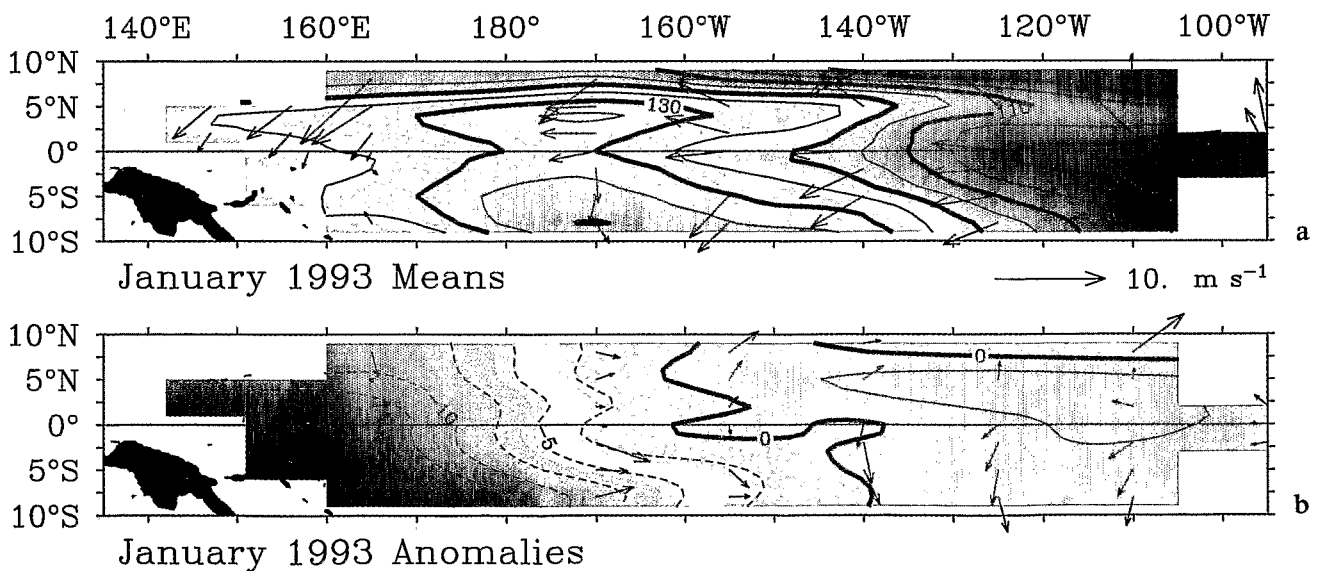


Plate 4. (a) Monthly mean dynamic height and (b) dynamic height anomaly for January 1993. Anomalies from the climatological January mean at mooring location have been gridded using an objective mapping procedure. The January mean represents the sum of the gridded anomalies plus the climatology. Overplotted are monthly mean wind vectors in Plate 4a and wind vector anomalies in Plate 4b.

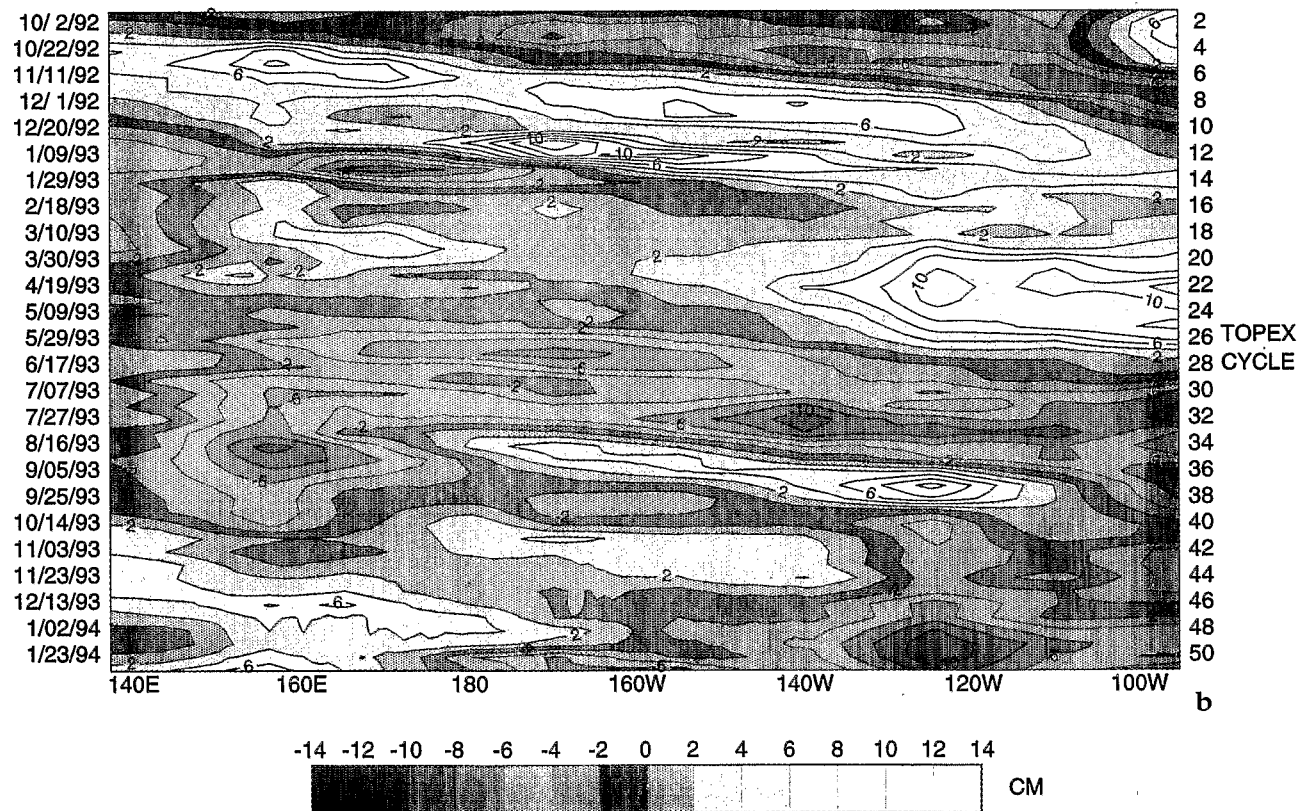
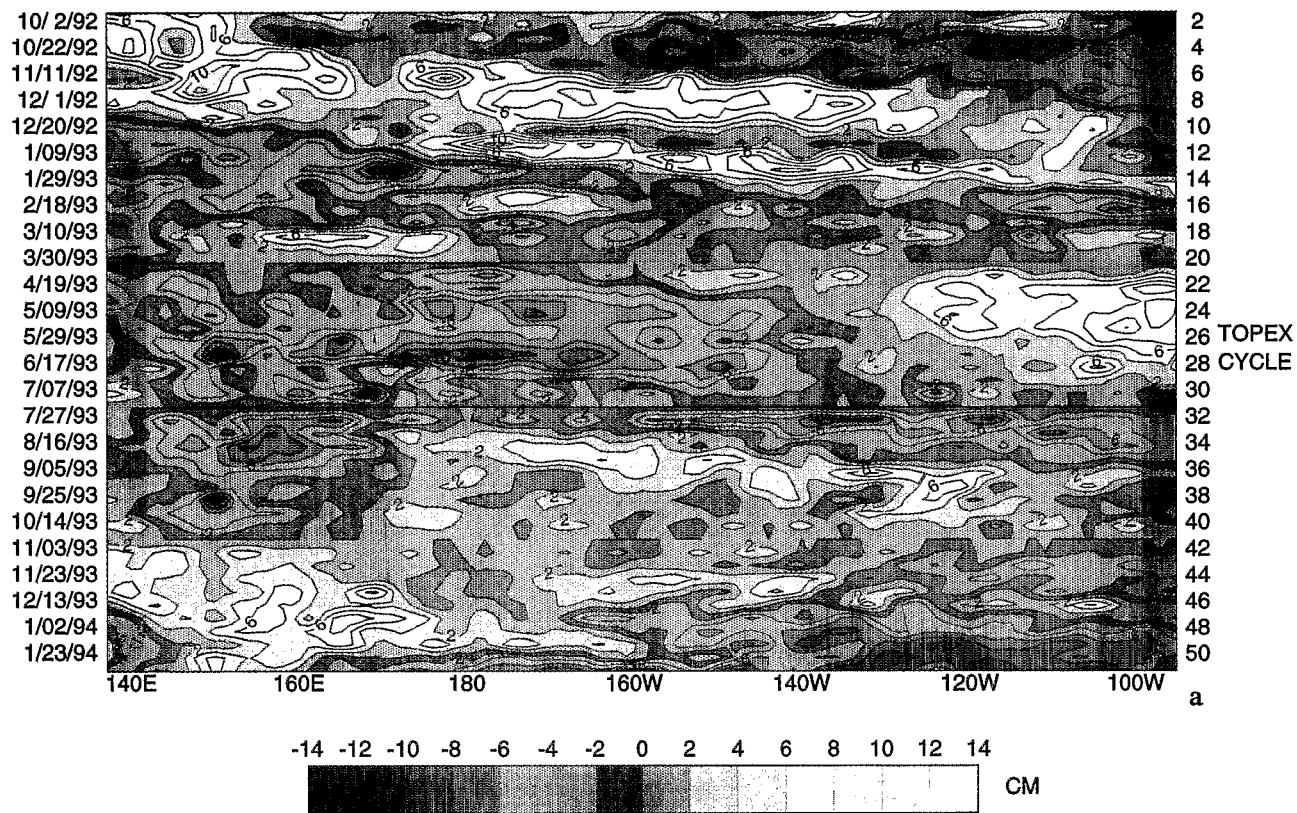


Plate 5. Time-longitude structure of surface topography variations along the equator from 137°E to 95°W. The 506-day mean has been removed from both data sets. (a) TOPEX sea level. (b) TOGA-TAO dynamic height (0/500 dbar). TOPEX data were not available during cycles 20, 31, and 41, when the POSEIDON altimeter was operating.

ary 13, 1994). This filters out some of the interannual variability (i.e., those changes in time coherent over these 500 days) discussed in the previous section; on the other hand, it does not filter out the seasonal cycle in either data set. Thus details of the anomaly structures discussed below may be quantitatively different than those described in section 3. However, referencing anomalies to the mean over 506 days allows for a consistent treatment of the two data sets and does not qualitatively affect identification of various wave modes in this study.

Plate 5 depicts the time-longitude structure of the equatorial sea surface topography variability relative to the 506-day mean. Similar eastward propagating features are present in both the TOPEX (Plate 5a) and TAO (Plate 5b) data sets. The amplitude of the variability is similar in both data sets, with TOPEX indicating more small-scale structure. This may be indicative of the fact that the TOPEX data have a greater spatial resolution than the TAO array. The phase lines in these time-longitude analyses imply eastward propagation speeds of $(2.49 \pm 0.22 \text{ m s}^{-1})$ for TOPEX and $(2.16 \pm 0.43 \text{ m s}^{-1})$ for TAO, which are consistent with the expected phase speeds of low-order baroclinic mode, equatorially trapped Kelvin waves.

Many of the same Kelvin wave features identified in the TAO data in section 3 are evident in the TOPEX data set as well. In response to the easterly wind anomalies east of 170°E in October 1992 (Plate 2a), depressed sea level associated with an upwelling Kelvin wave is seen to propagate east of 180° from the beginning of the TOPEX data to November 1992 (Plate 5a). As mentioned below, this same depression of sea level at the equator may induce a westward propagating response off the equator upon reflection at the eastern boundary. At the same time, but farther to the west, a downwelling Kelvin wave is being excited by a westerly wind burst that began near 165°E in late October. This coherent elevation of sea level is seen to propagate eastward in the TOPEX data to 130°W with amplitude $>6 \text{ cm}$. This is followed by a second westerly wind burst at the end of 1992 that, in turn, forces another downwelling Kelvin wave that propagates east of the dateline to 95°W . Note that for both downwelling Kelvin wave events there is a clear degradation in amplitude east of 130°W in both the TOPEX and TAO data sets. Similar behavior was also detected in Geosat and was attributed to the influence of upwelling favorable winds in the eastern portion of the basin [duPenhoat et al., 1992]. The presence of 2-m s^{-1} easterly wind anomalies in this region during December 1992 to March 1993 (Plate 2a) suggests this destructive interference may be at work again.

In mid-January 1993, easterly wind anomalies in the far western Pacific generate a sea level depression that propagates from 137°E , through the COARE domain [Eldin et al., 1994], to at least 140°W . During April and May both data sets depict a period of elevated sea level of 6–10 cm east of 130°W . This episode coincides with a 2-m s^{-1} relaxation of the equatorial easterlies near 145°W in April which may also be responsible for the off-equatorial response discussed below. In May–June both data sets indicate depressed sea from 160°E to 140°W at a time of easterly wind anomalies in the same region. A few months later, in July and August, another upwelling event spans most of the equatorial basin. This is followed by a 4-m s^{-1} westerly wind anomaly west of the date line in August and, subsequently during September,

an eastward propagation of elevated sea level east of the date line.

Although the time-longitude analysis along the equator is helpful for identifying eastward propagating, equatorially trapped Kelvin waves, westward propagating features are often identified by repeating the time-longitude analysis along latitudes other than the equator. Plate 6 presents the time-longitude structure of TOPEX and TAO surface topography variations along 5°N . This latitude was chosen because it is near the latitude of the peak amplitude of westward propagating, first baroclinic, first meridional mode Rossby waves, because there are 10 TAO moorings along this latitude, and because 5°N is also far enough north of the equator not to be significantly influenced by Kelvin waves. The time-longitude structure of both data sets is characterized by positive sea level anomalies east of the date line during the first 16 cycles, negative anomalies for the next 16 cycles, followed by positive anomalies for the last one third of the record. In terms of phase propagation the TOPEX data depict a series of small-scale westward propagating features between 120°W and 170°W during late 1992 to early 1993 and an apparent resumption during late 1993 to early 1994. The westward phase speed of these sea level changes is $\sim 45 \text{ cm s}^{-1}$, with a period of 20–30 days. Both the speed and period are inconsistent with first-mode Rossby waves. Rather, these oscillations are suggestive of the sea level expression of tropical instability waves that have been detected previously in Geosat altimeter data [Perigaud, 1990], advanced very high resolution radiometer data [Legeckis, 1977], and in situ data [Philander et al., 1985; Halpern et al., 1988]. It is worth noting in the TOPEX data that during the passage of the large sea level depression in the middle of the record it is hard to detect the presence of the instability waves. There is little evidence of the small-scale propagation in the TAO data because the 15° zonal spacing is not well suited for resolving the $\sim 1000\text{-km}$ zonal wavelength of these waves. However, the TAO data do depict the same large-scale sequence of positive, negative, positive sea level changes.

Even though the small-scale 20–30 day instability waves propagate westward at $\sim 45 \text{ cm s}^{-1}$, a lagged correlation analysis of the large-scale structure indicates the mean phase speed along 5°N for the entire record is westward, $-0.84 \pm 0.36 \text{ m s}^{-1}$ for TOPEX and $-0.89 \pm 0.29 \text{ m s}^{-1}$ for TAO. This faster overall phase speed is similar to that expected from linear theory for a first baroclinic, first meridional mode, equatorial Rossby wave, and is determined to a great extent by the large-scale westward propagating upwelling signal that is most evident between cycles 14 and 38. At the eastern boundary, just prior to this, there is some indication in the TOPEX data that the negative sea level in October–November may be consistent with the reflection of the upwelling Kelvin wave identified in both Plates 5a and 5b during the first few months of the mission. Thereafter, this upwelling signal reaches its maximum west of 140°W in late April to early May and may be related to the relaxation of the equatorial easterlies in this region (120°W – 160°W) that gave rise to the elevated sea level along the equator to the east. The timing of this upwelling Rossby wave is also consistent with the annual Rossby wave induced by wind stress curl changes north of the equator discussed by Kessler [1990]. Whether or not the relaxation of the equatorial easterlies seen here has a corresponding upwelling favorable wind

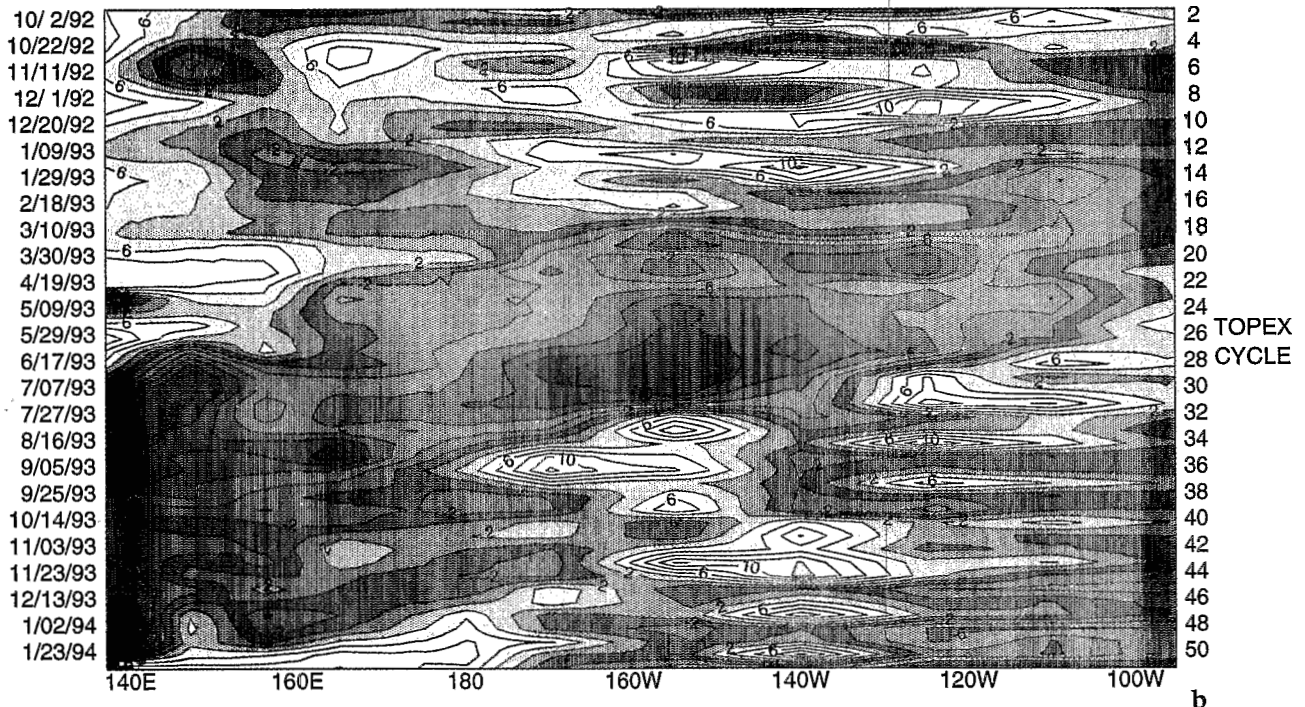
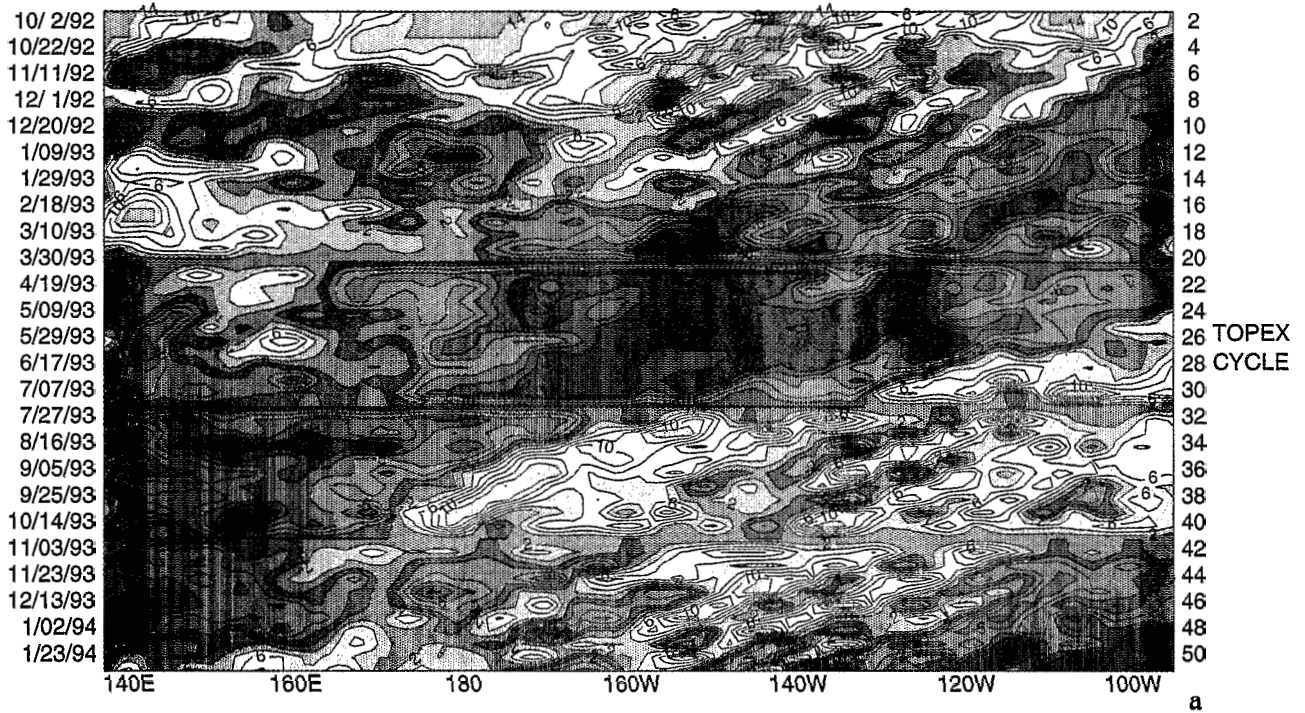


Plate 6. Time-longitude structure of surface topography variations along 5°N. (a) TOPEX sea level. (b) TOGA-TAO dynamic height (0/500 dbar).

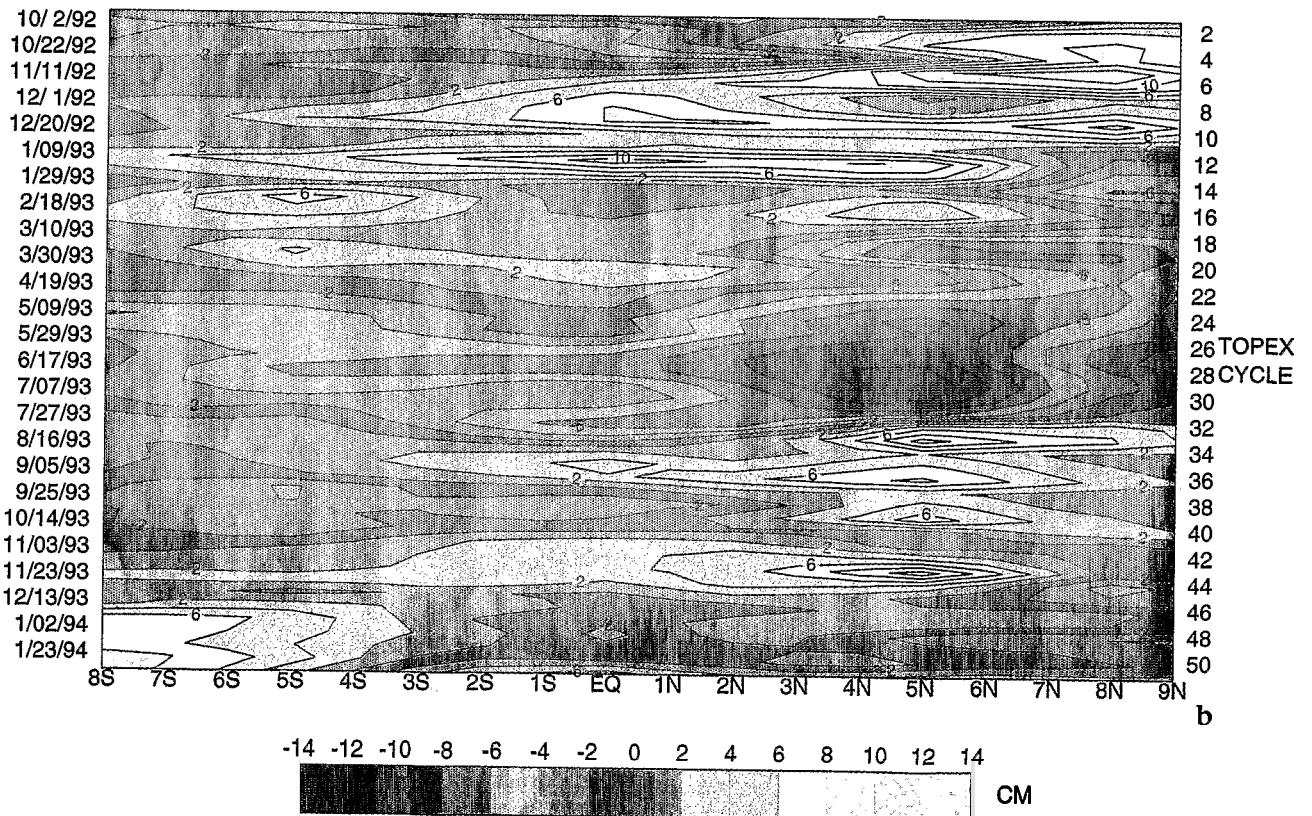
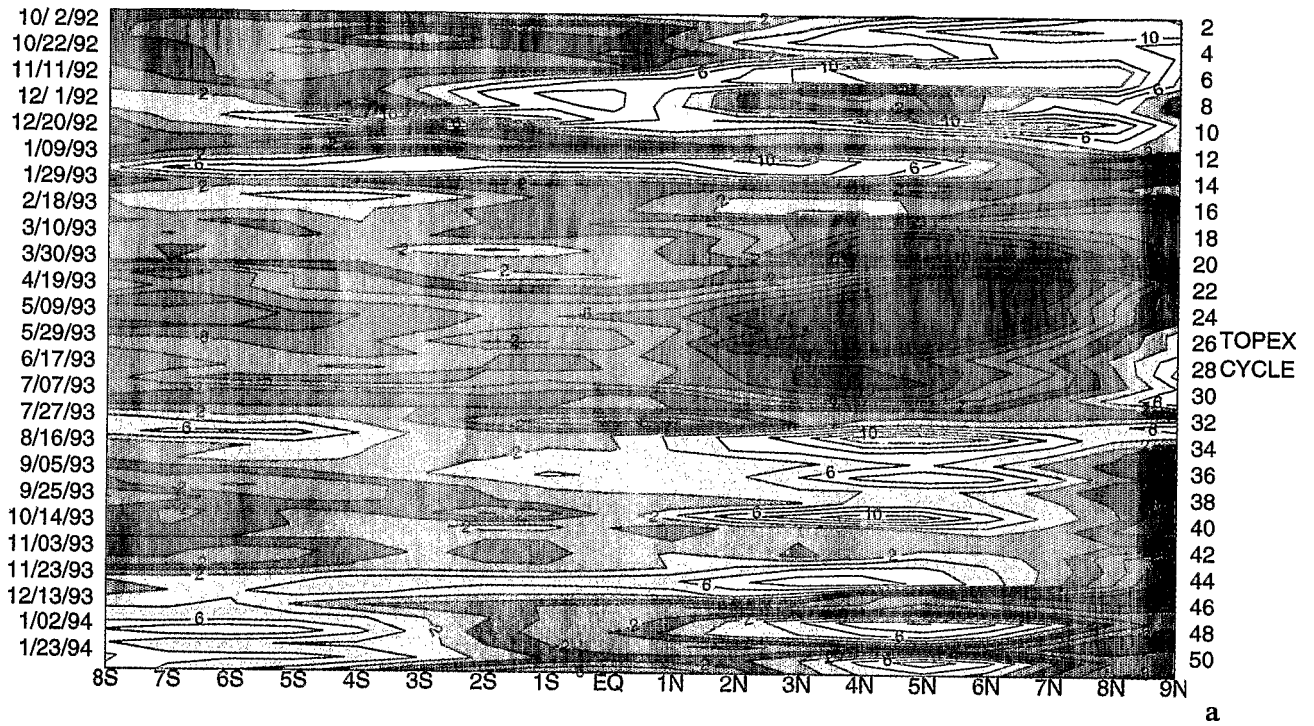


Plate 7. Time-latitude structure of surface topography variations along 155°W. (a) TOPEX sea level. (b) TOGA-TAO dynamic height (0/500 dbar).

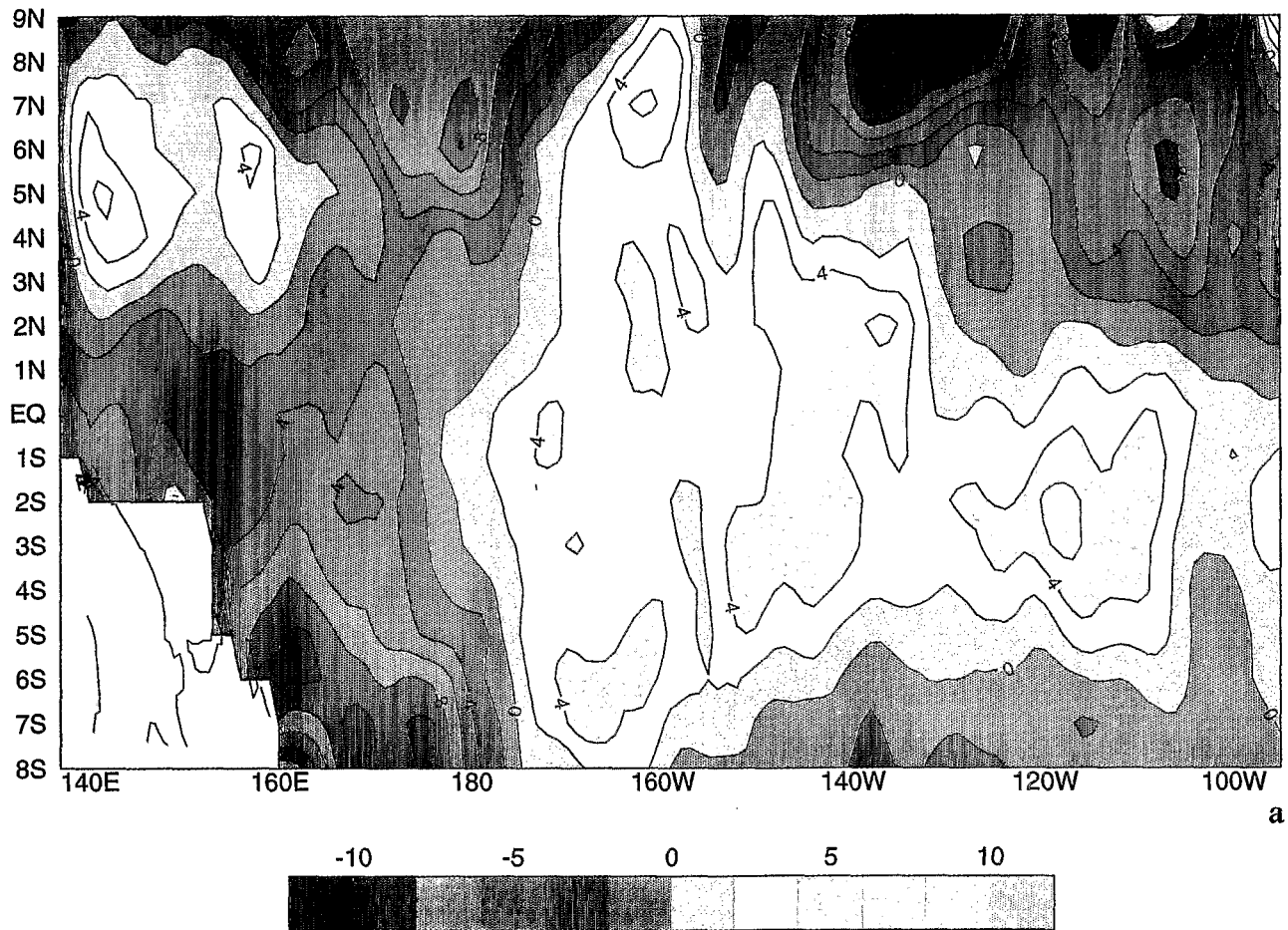


Plate 8. January 1993 monthly mean sea surface topography relative to the 506-day mean. (a) TOPEX sea level. (b) TOGA-TAO dynamic height (0/500 dbar).

stress pattern north of the equator has yet to be determined. After the passage of this drop in sea level, elevated sea level reappeared at the eastern boundary in both data sets during May 1993 and began to progress westward. The propagation of this elevated sea level away from the eastern boundary followed the appearance of the 6- to 10-cm elevation of sea level on the equator at the eastern boundary in April and May.

The meridional structure in the two data sets is depicted by a time-latitude plot along 155°W (Plate 7). This longitude was chosen because it is near the center of the basin and there are five to seven TAO moorings operating along this meridian during cycles 1–51. The maximum sea level variability in the two data sets is north of the equator with amplitudes of 8–14 cm. For the largest of these episodes in the TOPEX data, e.g., November–December 1992, January–February 1993, May–July 1993, there is a corresponding but smaller sea level change in the southern hemisphere as well. The same applies to a lesser extent in the TAO data. In particular, the possible expression of a westward propagating Rossby wave, denoted by the east to west sea level depressions in 1993 in Plate 6, reaches 155°W during May–July. At this time both the TOPEX and TAO data indicate negative sea level anomalies north and south of the equator. However, the 3° meridional decorrelation scale used in the optimal interpolation mapping and gaps in the mooring time

series due to occasional instrumental failures yield elongated meridional scales that preclude further discrimination of Rossby wave structures in this report.

As an example of the spatial correspondence of the two data sets, the monthly mean sea level structure for January 1993 is given in Plate 8. This is the time when the time-longitude analyses along the equator show that the second downwelling Kelvin wave was in the central Pacific, and the time-latitude analysis along 155°W indicates positive sea level between 8°N and 8°S. The spatial structure during January 1993 contains a large, positive sea level anomaly in the central and eastern Pacific surrounded by depressed sea level elsewhere in both data sets. In this representation there is no clear maximum centered on the equator, and the meridional scale is broader than expected for an equatorial Kelvin wave alone. Inspection of higher temporal resolution 10-day maps and time-latitude analyses farther to the west suggests that this broad, meridional positive sea level may be the superposition of the eastward propagating, downwelling Kelvin wave (as seen in Plate 5) and a westward propagating Rossby wave. The two combine to elevate sea level between ~6°N and 8°S.

Although most of the analyses to this point have focused on the space-time structure within the two data sets, the overall fidelity between the sea level variability of TOPEX and TAO is summarized by cross correlations and RMS

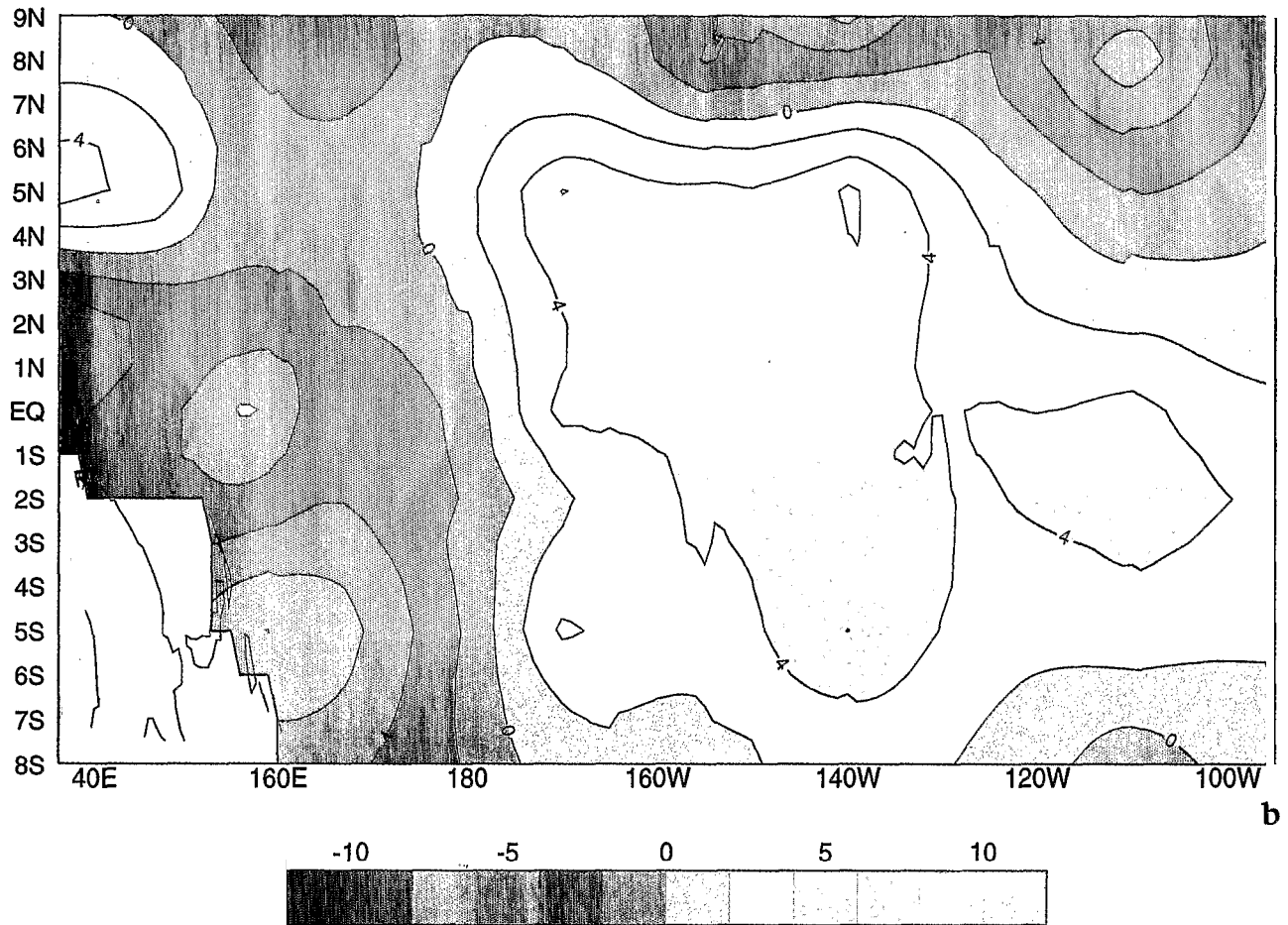


Plate 8. (continued)

differences (Plate 9). To assist in the interpretation, the locations of the TOGA-TAO moorings are shown on the correlation and RMS plots. In the central and western tropical Pacific and eastern equatorial Pacific there are large regions where the correlation is between 0.7 and 0.9 with RMS differences <4 cm. This is consistent with the general qualitative agreement noted in the previous time-longitude and time-latitude analyses. The greatest discrepancies between TOPEX and TAO are present in the northern and eastern tropical Pacific. In the east the correlations are often <0.5 off the equator. North of the equator, the RMS differences are often >5 cm. It is also worth noting that basin wide, the locations of the lowest correlations and highest RMS differences are found between the TAO mooring sites, suggesting that the optimal interpolation technique we have used to map the two data sets is interpolating dynamic height "information" between the moorings that differs from the TOPEX observations there.

5. Summary and Discussion

With the recent deployment of more than 60 TOGA-TAO moorings in the equatorial Pacific we have been able to do a quick look comparison between the 0/500 dbar dynamic height and sea level estimated from the TOPEX altimeter during the first 506 days of the TOPEX/POSEIDON mission. This intercomparison was facilitated through the optimal

interpolation of both sea level fields (relative to the 506-day mean) onto a common, 10-day, $1^\circ \times 1^\circ$ grid.

During the verification phase the TOPEX altimeter captured the major sea level signals associated with the continuation of the 1991–1993 El Niño event. These sea level signals, though significant, were smaller than those observed by the Geosat altimeter during the 1986–1987 El Niño [Cheney and Miller, 1988; Miller *et al.*, 1988; Delcroix *et al.*, 1991]. Overall, the TOPEX sea level contained more small-scale structure than the TOGA-TAO sea level, as evidenced by the detection of the instability waves in the eastern equatorial Pacific. The largest amplitude sea level variability was evident during the first 30 cycles and appeared to be related to a train of downwelling Kelvin waves, generated in boreal winter and spring by westerly winds in the western and central Pacific. These waves propagated all the way to the eastern Pacific, where they affected sea surface temperature [Kessler *et al.*, 1994] and may have contributed to the prolongation of the 1991–1993 El Niño event in the tropical Pacific. Along 5°N , both the data sets provide evidence of a westward propagating Rossby wave. The cause and effect of these wave features depicted in the TOPEX and TAO data sets is described in greater detail by J.-P. Boulanger and C. Menkes (manuscript in preparation, 1994).

Cross correlation between the two sea level fields was generally >0.7 , with an RMS difference <4 cm. However, in the eastern Pacific, cross correlations dropped significantly,

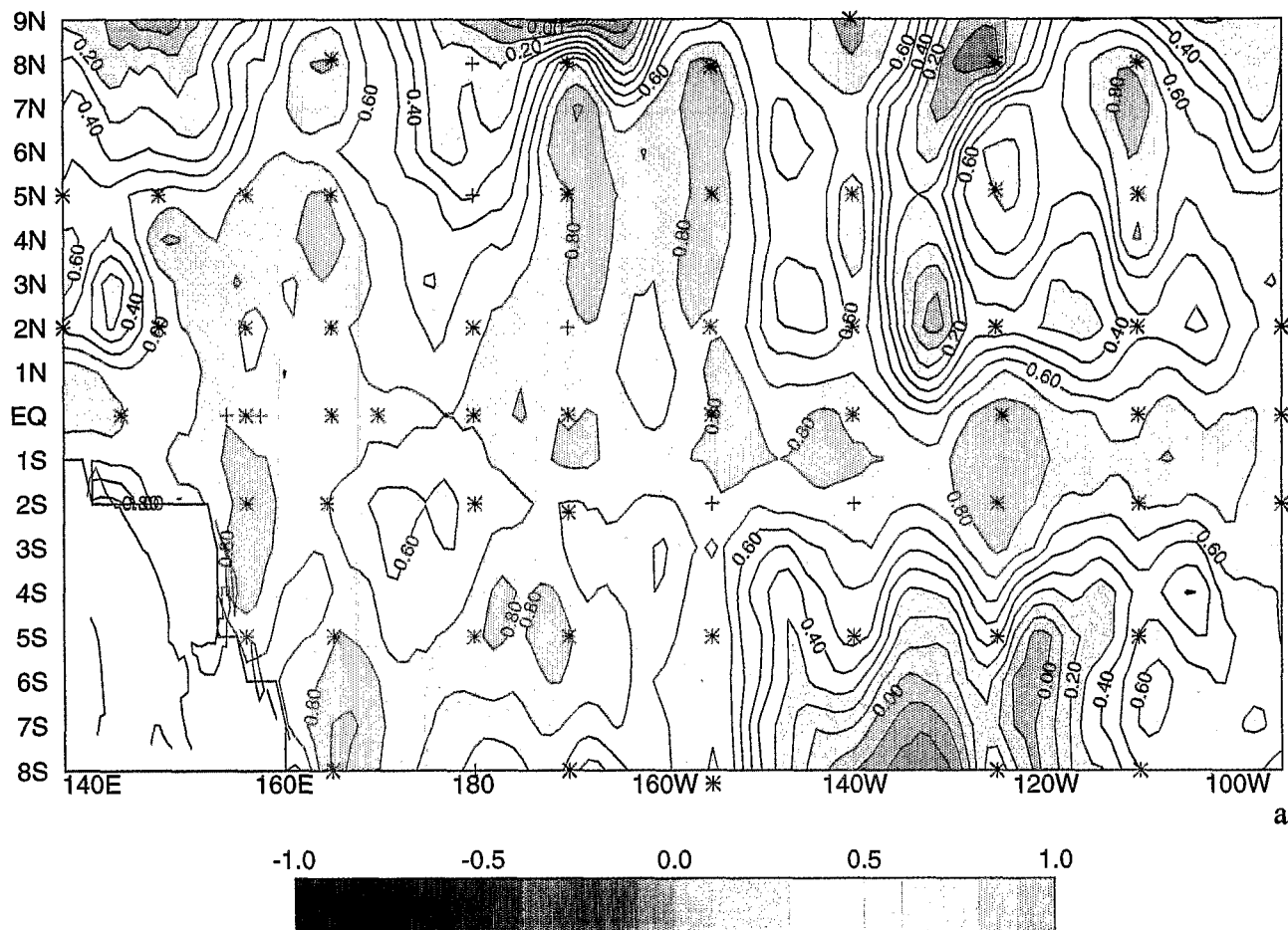


Plate 9. (a) Cross correlations between TOPEX and TOGA-TAO surface topographies (contour interval 0.1). (b) Root mean square differences between TOPEX and TOGA-TAO surface topographies (contour interval 1 cm). Mooring locations with >180 days of data during this period are indicated by asterisks; mooring locations with <180 days are indicated by pluses.

sometimes as low as 0.2, with RMS differences up to 7 cm. Such low correlations in the eastern Pacific were unexpected; they may be the result of a number of possibilities, e.g., poor temporal resolution of 20- to 30-day instability waves in the 10-day repeat TOPEX data, poor spatial resolution of the instability waves in the TAO data, imperfect water vapor retrieval over an area of strong and rapid sea surface temperature variations, or residual orbit error. Chief among the possible reasons for the discrepancies, however, may be error in the tidal corrections applied to the TOPEX data. *Schrama and Ray* [this issue] have demonstrated that the 10-day TOPEX sampling induces significant aliasing of the M_2 tide into a 62-day period band. In this study we removed the tidal effects as best we could using the corrections of *Ray et al.* [1994]. This tide model provided a noticeable improvement in our results near the equator in the eastern Pacific (correlations increased by 0.1 and 0.2 and RMS differences dropped by 1–2 cm) as compared when using the *Cartwright and Ray* [1990] and *Schwiderski* [1980] tide models. Yet, even after having applied the *Ray et al.* [1994] tides, there still remain unresolved discrepancies off the equator in the eastern equatorial Pacific. We would expect that comparisons between the two data sets will improve if the data are low-pass filtered for periods >60 days

in order to remove residual tidal errors and sampling errors pertaining to the instability waves.

Nevertheless, in both the TOPEX and TAO fields the observed signal over the 506-day period was generally greater (~2 times) than the expected measurement errors. In addition, the amplitude of the TOPEX sea level signal was of the same order as the TAO sea level signal. The unresolved systematic underestimation of altimeter sea level signals in the equatorial Pacific as observed by Geosat [*Cheney et al.*, 1989; *Delcroix et al.*, 1994] appears not to be an issue with TOPEX/POSEIDON.

This study is part of the preliminary analyses carried on during the verification phase of the TOPEX/POSEIDON mission. An initial intercomparison was made with the interim GDR sea level, only to reveal the poor quality of the interim product. However, the present GDR sea level needs to be more carefully processed if one wants to analyze sea level phenomena with a 4-cm accuracy (i.e., to resolve the meridional structure of equatorial waves) and to calculate currents (a major goal of the mission) in equatorial regions [*Picaut et al.*, 1990]. The ongoing data analysis of a dedicated validation experiment of TOPEX/POSEIDON altimeters using two ATLAS moorings in the western Pacific specifically deployed at TOPEX/POSEIDON crossover

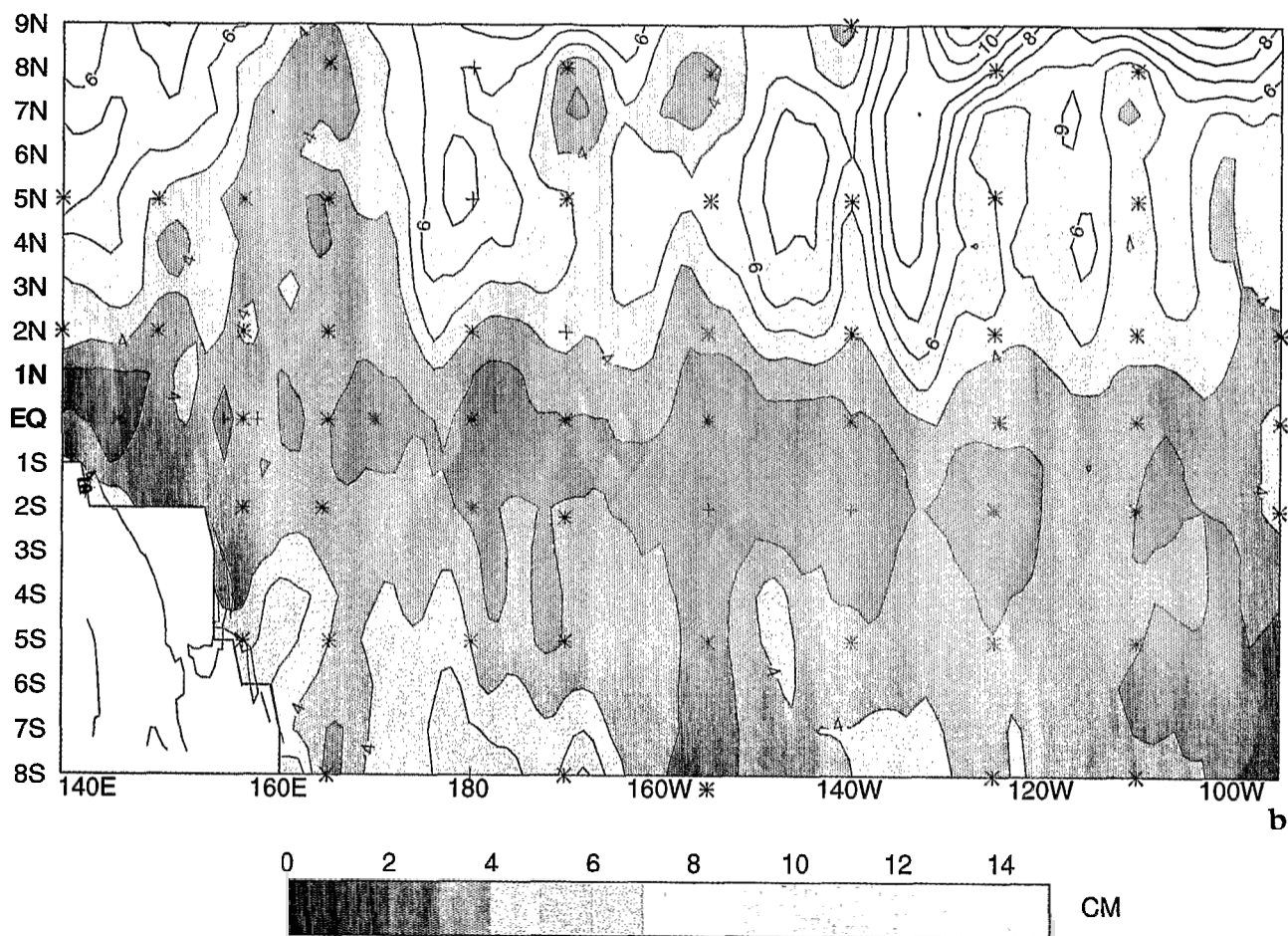


Plate 9. (continued)

points [Picaud *et al.*, 1992], together with careful individual sea level or current intercomparison at each TOGA-TAO mooring site, will help determine the best approach to processing the altimeter data, especially in terms of time-space decorrelation scales used in the optimal interpolation method.

These two in situ and remote sensing measurement technologies have their individual advantages, as well as unique logistical-deployment and lifetime limitations. The TOGA-TAO array has several advantages over the TOPEX/POSEIDON mission in terms of equatorial Pacific Ocean monitoring for climate purposes. TAO data provide greater temporal resolution, are transmitted in real time on the Global Telecommunication System, are multivariate, and are not restricted to surface variables only. Assimilation of these data in short-term climate forecast models may facilitate the prediction of major climatic events such as the El Niño-Southern Oscillation in the near future. On the other hand, satellite altimetry measurements provide denser spatial coverage and encompass most of the Pacific, Atlantic, and Indian Oceans. This spatial coverage should prove valuable in helping to determine the extra equatorial climatic influence, if any, of El Niño events. Although TOPEX/POSEIDON was designed as a research mission, including experimental sensor development (i.e., Poseidon altimeter), future improvements will have to be made in terms of rapid data processing and distribution before the data from subse-

quent altimeter missions can be used in an operational or near real-time mode. If sea level information is demonstrated to have a positive impact on climate prediction, e.g., as an initialization proxy for subsurface thermal structure, then a rigorous assessment of the relative importance of each monitoring approach could and should be made.

Acknowledgments. The authors wish to thank E. Hackert, D. McClurg, M. McCarty, and C. Menkes for their superb processing and analysis efforts with the TOPEX and TAO data sets. The special assistance rendered by B. Cliff and R. Martin is acknowledged. The authors are also very appreciative of the along-track TOPEX data provided to us by C. Koblinsky and his collaborators. This work was supported by NASA RTOP 578-21-03, the U.S.-TOGA Project Office, the NOAA/EPOCS program, and PNTS ASP 91N50/0550. The TOGA-TAO array is supported by the United States, Japan, France, Korea, and Taiwan.

References

- Cartwright, D. E., and R. D. Ray, Oceanic tides from Geosat altimetry, *J. Geophys. Res.*, **95**, 3069-3090, 1990.
- Cheney, R. E., and L. Miller, Mapping the 1986-1987 El Niño with Geosat altimeter data, *Eos Trans. AGU*, **69**, 754-755, 1988.
- Cheney, R. E., B. C. Douglas, and L. Miller, Evaluation of Geosat altimeter data with application to tropical Pacific sea level variability, *J. Geophys. Res.*, **94**, 4737-4748, 1989.
- Delcroix, T., J. Picaud, and G. Eldin, Equatorial Kelvin and Rossby waves evidenced in the Pacific Ocean through Geosat sea level and current anomalies, *J. Geophys. Res.*, **96**, 3246-3262, 1991.

- Delcroix, T., J.-P. Boulanger, F. Masia, and C. Menkes, Geosat-derived sea level and surface current anomalies in the equatorial Pacific during the 1986–1989 El Niño and La Niña, *J. Geophys. Res.*, **99**, 25,093–25,107, 1994.
- duPenhoat, Y., T. Delcroix, and J. Picaut, Interpretation of Kelvin/Rossby waves in the equatorial Pacific from model-GEOSAT data intercomparison during the 1986–1987 El Niño, *Oceanol. Acta*, **15**, 545–554, 1992.
- Eldin, G., T. Delcroix, C. Henin, K. Richards, Y. du Penhoat, J. Picaut, and P. Rual, Large-scale current and thermohaline structure along 156°E during the COARE Intensive Observation Period, *Geophys. Res. Lett.*, in press, 1994.
- Freitag, H. P., Y. Feng, L. J. Mangum, M. J. McPhaden, J. Neander, and L. D. Stratton, Calibration procedures and instrumental accuracy estimates of TOGA-TAO temperature, relative humidity and radiation measurements, *Tech. Memo.*, Natl. Oceanic and Atmos. Admin., Silver Spring, Md., in press, 1994.
- Fu, L.-L., and E. G. Christensen, TOPEX/POSEIDON performance evaluated, *Eos Trans. AGU*, **74**, 302, 1993.
- Halpern, D., R. A. Knox, and D. S. Luther, Observations of 20-day period meridional current oscillations in the upper ocean along the Pacific equator, *J. Phys. Oceanogr.*, **18**, 1514–1534, 1988.
- Hayes, S. P., L. J. Mangum, J. Picaut, A. Sumi, and K. Takeuchi, TOGA-TAO: A moored array for real-time measurements in the tropical Pacific Ocean, *Bull. Am. Meteorol. Soc.*, **72**, 339–347, 1991.
- Kessler, W. S., Observations of long Rossby waves in the northern tropical Pacific, *J. Geophys. Res.*, **95**, 5183–5217, 1990.
- Kessler, W. S., M. J. McPhaden, and K. Weickmann, Forcing of intraseasonal equatorial Kelvin waves, *J. Phys. Oceanogr.*, in press, 1994.
- Koblinsky, C. J., Ocean surface topography and circulation, in *Atlas of Satellite Observations Related to Global Change*, edited by R. Gurney, J. Foster, and C. Parkinson, pp. 223–236, Cambridge University Press, New York, 1993.
- Koblinsky, C. J., R. S. Nerem, R. G. Williamson, and S. M. Klosko, Global scale variations in sea surface topography determined from satellite altimetry, in *Sea Level Changes: Determination and Effects*, *Geophys. Monogr. Ser.*, vol. 69, edited by P. Woodworth, pp. 155–165, AGU, Washington, D. C., 1992.
- Kousky, V. E., The global climate of December 1991–February 1992: Mature phase warm (ENSO) episode conditions develop, *J. Clim.*, **6**, 1639–1655, 1993.
- Legeckis, R., Long waves in the eastern equatorial Pacific Ocean, A view from a geostationary satellite, *Science*, **197**, 1179–1181, 1977.
- Levitus, S., Climatological atlas of the world ocean, *NOAA Prof. Pap.* **13**, 173 pp., U.S. Govt. Print. Off., Washington, D. C., 1982.
- McCarty, M. E., and M. J. McPhaden, Mean seasonal cycles and interannual variations at 0°, 165°E during 1986–1992, *Tech. Memo. ERL PMEL-98*, 64 pp., Natl. Oceanic and Atmos. Admin., Silver Spring, Md., 1993.
- McPhaden, M. J., TOGA-TAO and the 1991–93 ENSO event, *Oceanography*, **6**, 36–44, 1993.
- McPhaden, M. J., H. B. Milburn, A. I. Nakamura, and A. J. Shepherd, PROTEUS—Profile telemetry of upper ocean currents, *Sea Technol.*, **32**, 10–19, 1991.
- Miller, L., R. E. Cheney, and B. C. Douglas, Geosat altimeter observations of Kelvin waves and the 1986–87 El Niño, *Science*, **239**, 52–54, 1988.
- Mitchum, G., Comparison of TOPEX sea surface heights with tide gauge sea levels, *J. Geophys. Res.*, this issue.
- Perigaud, C., Sea level oscillations observed with Geosat along two shear fronts of the Pacific North Equatorial Countercurrent, *J. Geophys. Res.*, **95**, 7239–7248, 1990.
- Philander, S. G. H., et al., Long waves in the equatorial Pacific Ocean, *Eos Trans. AGU*, **66**, 154, 1985.
- Picaut, J., A. J. Busalacchi, M. J. McPhaden, and B. Camusat, Validation of the geostrophic method for estimating zonal currents at the equator from Geosat altimeter data, *J. Geophys. Res.*, **95**, 3015–3024, 1990.
- Picaut, J., A. J. Busalacchi, T. Delcroix, and M. J. McPhaden, Rigorous open-ocean validation of TOPEX/POSEIDON sea level in the western equatorial Pacific, TOPEX/POSEIDON joint verification plan, *JPL Publ.*, **92–9**, 14–16, 1992.
- Ray, R. D., B. V. Sanchez, and D. E. Cartwright, Some extensions to the response method of tidal analysis applied to TOPEX/POSEIDON altimetry, *Eos Trans. AGU*, **75**(16), Spring Meeting Suppl., 108, 1994.
- Reynolds, R., A real-time global sea surface temperature analysis, *J. Clim.*, **1**, 75–86, 1988.
- Schrama, E. J. O., and R. D. Ray, A preliminary tidal analysis of TOPEX/POSEIDON altimetry, *J. Geophys. Res.*, this issue.
- Schwiderski, E. W., On charting global ocean tides, *Rev. Geophys.*, **18**, 243–268, 1980.
- Webster, P. J., and R. Lukas, TOGA-COARE: The Coupled Ocean-Atmosphere Response Experiment, *Bull. Am. Meteorol. Soc.*, **73**, 1377–1416, 1992.
- Woodruff, S. D., R. J. Slutz, R. L. Jenne, and P. M. Steurer, A comprehensive ocean-atmosphere data set, *Bull. Am. Meteorol. Soc.*, **68**, 1239–1250, 1987.
- Wyrtki, K., and B. Kilonsky, Mean water mass structure during the Hawaii-to-Tahiti Shuttle Experiment, *J. Phys. Oceanogr.*, **14**, 242–254, 1984.
- Wyrtki, K., and G. Mitchum, Interannual differences of Geosat altimeter heights and sea level: The importance of a datum, *J. Geophys. Res.*, **95**, 2966–2975, 1990.

A. J. Busalacchi, Laboratory for Hydrospheric Processes, NASA Goddard Space Flight Center, Mail Code 970, Greenbelt, MD 20771.
 M. J. McPhaden, Pacific Marine Environmental Laboratory, NOAA, Seattle, WA 98115.
 J. Picaut, Groupe SURTROPAC, ORSTOM, B.P. A5, Noumea, New Caledonia.

(Received November 29, 1993; revised June 21, 1994; accepted June 21, 1994.)